JOC Article

Esters of 5-Carboxyl-5-methyl-1-pyrroline *N*-Oxide: A Family of Spin Traps for Superoxide

Pei Tsai,[†] Kazuhiro Ichikawa,[‡,§,⊥] Colin Mailer,[‡,§] Sovitj Pou,[†] Howard J. Halpern,[‡,§] Bruce H. Robinson,[∥] Robert Nielsen,[∥] and Gerald M. Rosen*[,†,§]

Department of Pharmaceutical Sciences, University of Maryland School of Pharmacy, Baltimore, Maryland 21201, Medical Biotechnology Center, University of Maryland Biotechnology Institute, Baltimore, Maryland 21201, Department of Radiation and Cellular Oncology, The University of Chicago, Illinois 60637, Center for Low-Frequency EPR Imaging for In Vivo Physiology, The University of Chicago, Chicago, Illinois 60637, University of Maryland, Baltimore, Baltimore, Maryland 21201, and Department of Chemistry, University of Washington, Seattle, Washington 98195

grosen@umaryland.edu

Received July 18, 2003

Apparent rate constants, at acidic pH and neutral pH for the reaction of a family of ester-containing 5-carboxyl-5-methyl-1-pyrroline *N*-oxides with superoxide ($O_2^{\bullet-}$) were estimated, using ferricytochrome *c* as a competitive inhibitor. It was of interest to note that the rate constants were similar among the different nitrones and not that significantly different from that found for 5-(diethoxyphosphoryl)-5-dimethyl-1-pyrroline *N*-oxide. At acidic pH, the rate constant for spin trapping $O_2^{\bullet-}$ was 3-fold greater than that at physiological pH. Subsequent experiments determined the half-life of aminoxyls, derived from the reaction of these nitrones with $O_2^{\bullet-}$. The EPR spectra were modeled by using a global analysis method. The results clearly demonstrated that EPR spectra of all the aminoxyls were inconsistent with a model that included a single γ-hydrogen splitting. A better interpretation modeled them as two diastereomers with identical nitrogen splittings and slightly different β-hydrogen splittings. Detailed line width analyses slightly favored an equal line width−unequal population ratio for the two diastereomers.

Introduction

Spin trapping/EPR spectroscopy is one of the most reliable methods for identifying free radicals, especially in biological systems.[1] In fact, were it not for spin trapping, the observation that nitric oxide synthase (NOS; EC 1.14.13.39)[2] generates $O_2^{\bullet-}$ might have remained undiscovered for many years,[3] and H_2O_2 would have been considered the sole NOS reduction product of O_2.[4]

Since the late 1970s, 5,5-dimethyl-1-pyrroline *N*-oxide **1** has been the primary spin trap for $O_2^{\bullet-}$, owing this status to the unique 12-line EPR spectrum of aminoxyl **2**, arising from the reaction of $O_2^{\bullet-}$ with nitrone **1**.[5] Unfortunately, aminoxyl **2** has a short lifetime, decomposing into several compounds, one of which is aminoxyl **3**.[5b,6] Aminoxyl **3** can also arise from the reaction of nitrone **1** with $HO^{\bullet}$ (Scheme 1). Further, reaction of nitrone **1** with $O_2^{\bullet-}$ is slow, at ∼15 M^{-1} s^{-1} at pH 7.0.[6a] Finally, nitrone **1** is susceptible to a variety of oxidative reactions,[6b,7] thereby further limiting its utility as a spin trap for $O_2^{\bullet-}$ in biological milieu.

Attempts to improve the reactivity of nitrones toward $O_2^{\bullet-}$ through the inclusion of different substituents on

* Address correspondence to Gerald M. Rosen at the University of Maryland School of Pharmacy. Phone: 410-706-0514. Fax: 410-706-8184.

[†] University of Maryland School of Pharmacy and University of Maryland Biotechnology Institute.

[‡] Department of Radiation and Cellular Oncology, The University of Chicago.

[§] Center for Low-Frequency EPR Imaging for In Vivo Physiology, The University of Chicago, and the University of Maryland.

[⊥] On leave from Kyushu University, Fukuoka, Japan.

[∥] University of Washington.

(1) (a) There are a large number of review articles on this subject. For a classical paper on this topic, see: Janzen, E. G. *Acc. Chem. Res.* **1971**, *4*, 31−40. (b) Finkelstein, E.; Rosen, G. M.; Rauckman, E. J. *Arch. Biochem. Biophys.* **1980**, *200*, 1−16.

(2) Stuehr, D. J.; Kwon, N. S.; Nathan, C.; Griffith, O. W.; Feldman, P. L.; Wiseman, J. *J. Biol. Chem.* **1991**, *266*, 6259−6263.

(3) (a) Pou, S.; Pou, W. S.; Bredt, D. S.; Snyder, S. H.; Rosen, G. M. *J. Biol. Chem.* **1992**, *267*, 24173−24176. (b) Xia, Y.; Roman, L. J.; Masters, B. S. S.; Zweier, J. L. *J. Biol. Chem.* **1998**, *273*, 22635−22639. (c) Vásquez-Vivar, J.; Kalyanaraman, B.; Martásek, P.; Hogg, N.; Masters, B. S. S.; Karoui, H.; Tordo, P.; Pritchard, K. A., Jr. *Proc. Natl. Acad. Sci. U.S.A.* **1998**, *95*, 9220−9225. (d) Xia, Y.; Tsai, A.-L.; Berka, V.; Zweier, J. L. *J. Biol. Chem.* **1998**, *273*, 25804−25808. (e) Pou, S.; Keaton, L.; Surichamorn, W.; Rosen, G. M. *J. Biol. Chem.* **1999**, *274*, 9573−9580. (f) Vásquez-Vivar, J.; Hogg, N.; Martásek, P.; Karoui, H.; Pritchard, K. A., Jr.; Kalyanaraman, B. *J. Biol. Chem.* **1999**, *274*, 26736−26742. (g) Tsai, P.; Porasuphatana, S.; Pou, S.; Rosen, G. M. *J. Chem. Soc., Perkin Trans.* **2000**, *2*, 983−988. (h) Yoneyama, H.; Yamamoto, A.; Kosaka, H. *Biochem. J.* **2001**, *360*, 247−253. (i) Vásquez-Vivar, J.; Martásek, P.; Whitsett, J.; Joseph, J.; Kalyanaraman, B. *Biochem. J.* **2002**, *362*, 733−729.

(4) (a) Mayer, B.; John, M.; Heinzel, B.; Werner, E. R.; Wachter, H.; Schultz, G.; Böhme, E. *FEBS Lett.* **1991**, *288*, 187−191. (b) Heinzel, B.; John, M.; Klatt, P.; Böhme, E.; Mayer, B. *Biochem. J.* **1992**, *281*, 627−630.

(5) (a) Harbour, J. R.; Chow, V.; Bolton, J. R. *Can. J. Chem.* **1974**, *52*, 3549−3553. (b) Finkelstein, E.; Rosen, G. M.; Rauckman, E. J. *Mol. Pharmacol.* **1979**, *16*, 676−685.

(6) (a) Finkelstein, E.; Rosen, G. M.; Rauckman, E. J. *J. Am. Chem. Soc.* **1980**, *102*, 4994−4999. (b) Makino, K.; Hagi, A.; Ide, H.; Murakami, A.; Nishi, M. *Can. J. Chem.* **1992**, *70*, 2818−2827. (c) Hanna, P. M.; Chamulitrate, W.; Mason, R. P. *Arch. Biochem. Biophys.* **1992**, *296*, 640−644.

10.1021/jo0350413 CCC: $25.00
Published on Web 08/30/2003

SCHEME 1

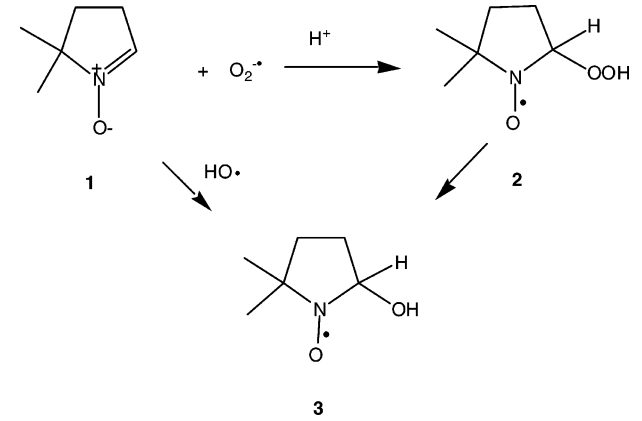

SCHEME 2

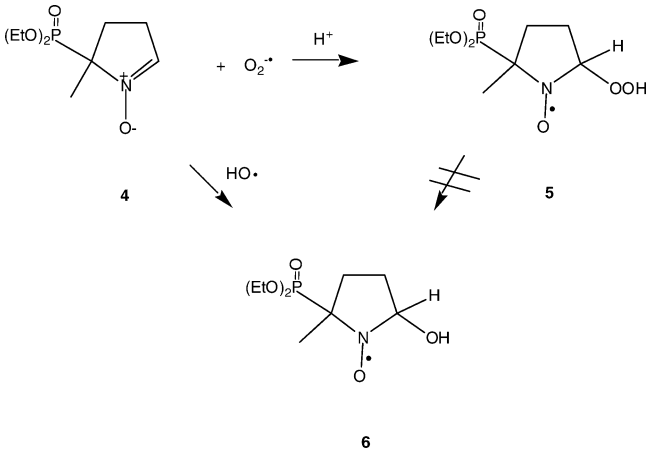

the pyrroline *N*-oxide ring have produced some success.[8] For instance, 5-(diethoxyphosphoryl)-5-dimethyl-1-pyrroline *N*-oxide **4**,[8c,e] reacts with $O_2^{\bullet-}$ at 80 M^{-1} s^{-1} at pH 7.0, affording aminoxyl **5**, whose half-life is about 18 min (Scheme 2).

However, difficulties encountered isolating pure nitrone **4**[8f] have, not surprisingly, sparked considerable interest in the synthesis of other cyclic nitrones. For instance, several contemporary papers[9a−d] described the spin trapping of $O_2^{\bullet-}$ by 5-ethoxycarbonyl-5-methyl-1-pyrroline *N*-oxide **7** and 5-*tert*-butoxycarbonyl-5-methyl-1-pyrroline *N*-oxide **11** (Scheme 3). For nitrone **7**, the rate constant for the reaction of $O_2^{\bullet-}$ has not been determined, whereas for nitrone **11**, there are significantly different reported rate constants for the spin trapping of $O_2^{\bullet-}$.[9e,f] Given that there are limited kinetic data on the reaction

SCHEME 3

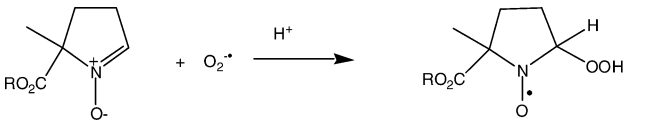

R = C_2H_5, **7**
R = CH_3, **8**
R = $CH_2(CH_2)_2CH_3$, **9**
R = $CH(CH_3)_2$, **10**
R = $C(CH_3)_3$, **11**
R = $CH_2CH(CH_3)_2$, **12**

R = C_2H_5, **13**
R = CH_3, **14**
R = $CH_2(CH_2)_2CH_3$, **15**
R = $CH(CH_3)_2$, **16**
R = $C(CH_3)_3$, **17**
R = $CH_2CH(CH_3)_2$, **18**

TABLE 1. EPR Hyperfine Splitting Constants for Spin Trapping $O_2^{\bullet-}$

aminoxyl	hyperfine splitting constants (at 9.5 GHz) A_N	A_H^{β}	% of the two isomers
[**13**]	13.13	11.66	59
	13.10	9.43	41
[**14**]	13.09	11.56	58
	13.09	9.30	42
[**15**]	13.13	11.56	57
	13.10	9.29	43
[**16**]	13.15	11.70	59
	13.13	9.44	41
[**17**]	13.23	11.79	59
	13.21	9.49	41
[**18**]	13.12	11.63	58
	13.10	9.34	42

of $O_2^{\bullet-}$ with ester-containing nitrones, it is difficult to predict, a priori, which of these spin traps is best suited for identifying $O_2^{\bullet-}$ in biological systems.

We, therefore, decided to determine rate constants for the reaction of $O_2^{\bullet-}$ toward nitrones **7**−**12**. We then estimated the half-life of aminoxyls **13**−**18** with the goal of determining which of these nitrones is the best of the next generation of spin traps for biologically generated $O_2^{\bullet-}$.

Results and Discussion

As we completed the writing of this manuscript, a recent paper[9c] appeared, disclosing the preparation of a family of ester containing 5-carboxyl-5-methyl-1-pyrroline *N*-oxides, most of which we had independently synthesized through a synthetic scheme that did not differ significantly from that of Stolze *et al.*[9c] 5-Methoxycarbonyl-5-methyl-1-pyrroline *N*-oxide **8** and 5-iso-butoxycarbonyl-5-methyl-1-pyrroline *N*-oxide **12** are unique to this paper.

Our experiments explored the spin trapping of $O_2^{\bullet-}$ by the esters of 5-carboxy-5-methyl-1-pyrroline *N*-oxides **7**−**12**. In our hands, EPR spectra of aminoxyls **13**−**18** were not that significantly different (Table 1). Of interest, however, is the suggestion that the EPR spectrum of aminoxyl **13** contains an A_H^{γ} hyperfine splitting,[9b] whereas

(7) (a) Makino, K.; Imaishi, H.; Morinishi, S.; Hagiwara, T.; Takeuchi, T.; Murakami, A. *Free Radical Res. Commun.* **1989**, *6*, 19−28. (b) Makino, K.; Hagiwara, T.; Hagi, A.; Nishi, M.; Murakami, A. *Biochem. Biophys. Res. Commun.* **1990**, *172*, 1073−1080.

(8) (a) Turner, M. J., III; Rosen, G. M. *J. Med. Chem.* **1986**, *29*, 2439−2444. (b) Rosen, G. M.; Tuner, M. J., III *J. Med. Chem.* **1988**, *31*, 428−232. (c) Fréjaville, C.; Karoui, H.; Tuccio, B.; Le Moigne, F.; Culcasi, M.; Pietri, S.; Laruicella, R.; Tordo, P. *J. Chem. Soc., Chem. Commun.* **1994**, 1793−1794. (d) Sankurati, N.; Janzen, E. G. *Tetrahedron Lett.* **1996**, *37*, 5313−5316. (e) Olive, G.; Le Moigne, F.; Mercier, A.; Rockenbauer, A.; Tordo, P. *J. Org. Chem.* **1998**, *63*, 9095−9099. (f) Barbati, S.; Clément, S.-L.; Fréjaville, C.; Bouteiller, J.-C.; Tordo, P.; Michel, J.-C.; Yadan, J.-C. *Synthesis* **1999**, 2036−2040. (g) Karoui, H.; Nsanzumuhire, C.; Le Moigne, F.; Tordo, P. *J. Org. Chem.* **1999**, *64*, 1471−1477. (h) Xu, Y.-K.; Chen, Z.-W.; Sun, J.; Shi, W.; Wang, H.-M.; Liu, Y. *J. Org. Chem.* **2000**, *67*, 7624−7630.

(9) (a) Olive, G.; Mercier, A.; Le Moigne, F.; Rockenbaur, A.; Tordo, P. *Free Radicals Biol. Med.* **2000**, *28*, 403−408. (b) Zhang, H.; Joseph, J.; Vasquez-Vivar, J.; Karoui, H.; Nsanzumuhire, C.; Martásek, P.; Tordo, P.; Kalyanaraman, B. *FEBS Lett.* **2000**, *473*, 58−62. (c) Stolze, K.; Udilova, N.; Rosenau, T.; Hofinger, A.; Nohl, H. *Biol. Chem.* **2003**, *384*, 493−500. (d) Zhao, H.; Joseph, J.; Zhang, H.; Karoui, H.; Kalyanaraman, B. *Free Radicals Biol. Med.* **2001**, *31*, 599−606. (e) Rosen, G. M.; Tsai, P.; Weaver, J.; Porasuphatana, S.; Roman, L. J.; Starkov, A. A.; Fiskum, G.; Pou, S. *J. Biol. Chem.* **2002**, *277*, 40275−40280. (f) Villamena, F. A.; Zweier, J. L. J. *Chem. Soc., Perkin Trans. 2* **2002**, 1340−1344.

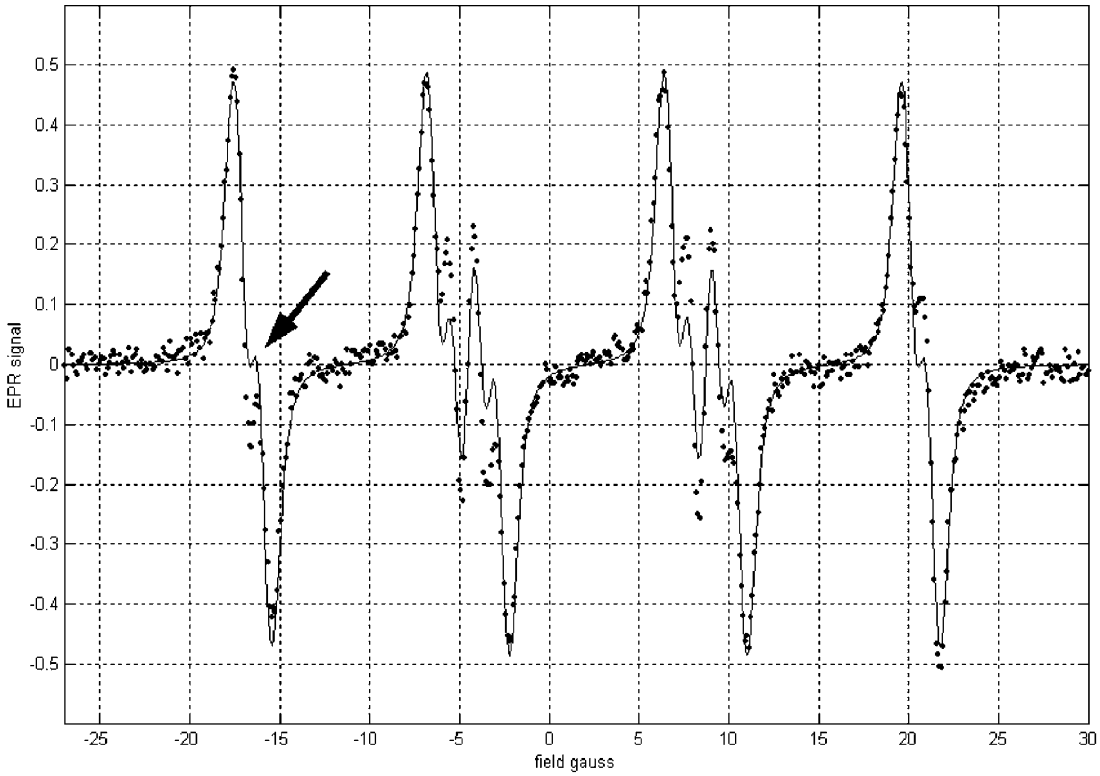

FIGURE 1. EPR spectrum of aminoxyl **17** fitted with a model that assumes there is only one species with hyperfine splittings: $A_N = 13.22$ G, $A_H{}^{\beta} = 10.74$ G, and $A_H{}^{\gamma} = 1.1$ G. Parameters that were allowed to float were the Lorentzian line width, the spectrum center, the scale factor determining the amplitude of the fitted spectrum, and the microwave phase of the bridge. The unresolved hyperfine structure from the four ^{1}H's at C-3 and C-4 and the three methyl ^{1}H's was modeled by assuming a hyperfine splitting of 0.2 G. The arrow shows one of the small features discussed in the text. The dots are experimental data, and the solid line is fitted data.

other reports[9a,c,d] propose that for aminoxyls **13**, and **15**−**17**, the EPR spectrum can be assigned to two diastereomers, absent of any $A_H{}^{\gamma}$ hyperfine splitting.[9c] Given that aminoxyls have very similar EPR spectra (Table 1), we inquired as to which model best describes these experimental data.

Line Width Analysis

Several possibilities were considered to explain the EPR spectra of aminoxyls **13**−**18**. First, that the γ-splitting arose from one of the hydrogen atoms at either carbon 3 or carbon 4 of aminoxyls **13**−**18** (Scheme 3). Here, electron spin density on one of the hydrogen atoms might be sufficient to split the electron energy levels. The question as to why, or how, only one hydrogen atom has this effect has not been addressed.[9b.] There are four hydrogen atoms at the 3 and the 4 positions: Why should only one of them contribute to the γ-splitting? Second, the 12-line EPR spectrum could be explained as a sum of two diastereomers of aminoxyls **13**−**18**. Published data obtained at X-band suggest that the EPR spectrum contains slightly unequal populations of the two diastereomers.[9a,9d]

The answers to these questions lie in the subtle details of the EPR spectrum. To fully explain these details it is crucial to accurately model everything that affects the shape of the spectrum. This includes modeling the distorting effects of the acquisition conditions, viz., over modulation and power broadening effects. To this end, we modified the algorithms of Robinson et al.[10] developed for the single nitroxide spectrum to fit EPR spectra with different populations of contributing aminoxyls. An important feature of the program is that it allows the linkage of parameters. For example, the widths or intensities of spectral lines of a set of spectra can be forced to be equal, even though the actual values of the line width or intensity are not known a priori.

We chose to evaluate the EPR spectrum of the smallest ester, e.g., aminoxyl **14**, and the bulkiest ester, e.g., aminoxyl **17**. The findings were the same. For illustrative purposes, we show the results of fitting the EPR spectrum of aminoxyl **17** with three different models (Figures 1−3). Model 1 predicts that the EPR spectrum is an average of the different diastereomers with hyperfine splittings of 13.22 G for ^{14}N, 10.74 G for the ^{1}H at the 2-position, and 1.14 G from a single ^{1}H splitting at either the 3- or the 4-position (Figure 1). Immediate and obvious restrictions apply to the apparent line widths for this model: they *must* be equal. In addition, the two 6-line spectra resulting from the γ-^{1}H split *must* have equal intensities. Figure 1 shows the experimental EPR spectrum (dots) overlaid with the best-fit simulation of Model 1. The line width and intensity restrictions mandate that the small features arising from partial resolution (at, for

(10) (a) Robinson, B. H.; Mailer, C.; Reese, A. W. *J. Magn. Reson.* **1999**, *138*, 199−200. (b) Robinson, B. H.; Mailer, C.; Reese, A. W. *J. Magn. Reson.* **1999**, *138*, 210−219. (c) Mailer, C.; Robinson, B. H.; Williams, B. B.; Halpern, H. J. *Magn. Reson. Med.* **2003**, *49*, 1175−1180.

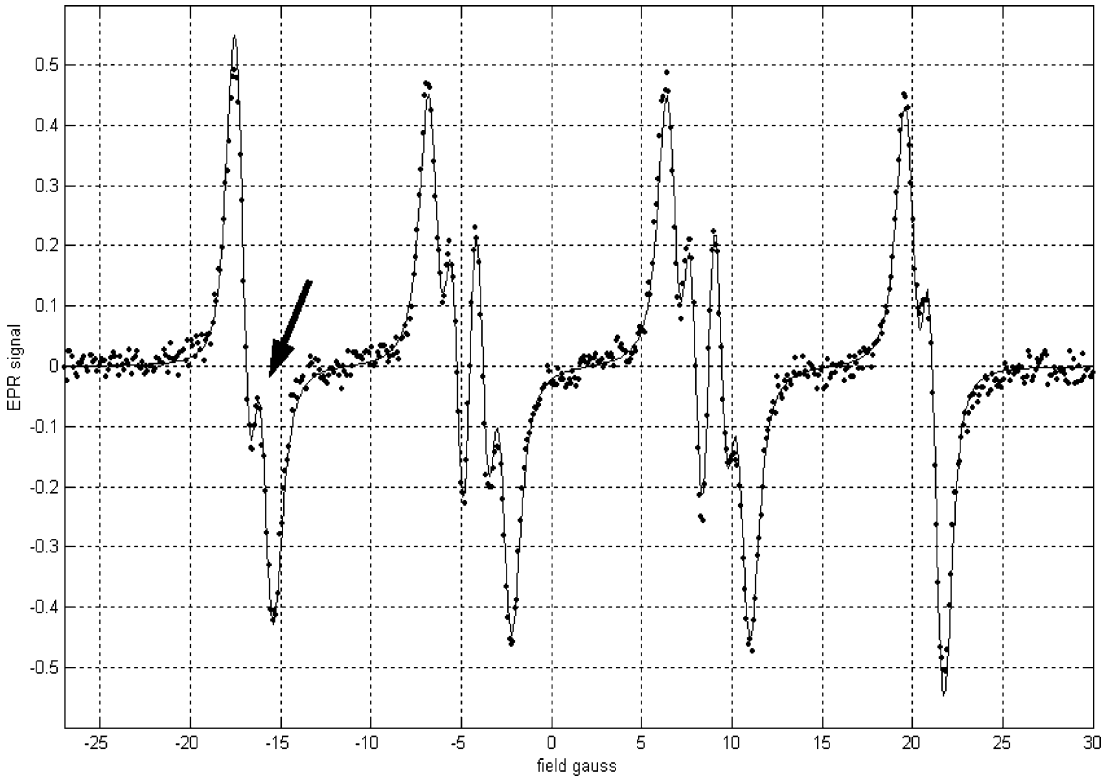

FIGURE 2. EPR spectrum of aminoxyl **17** fitted with a model that assumes there are two diastereomers with equal populations but with the individual Lorentzian line widths allowed to float. Fitted parameters were as follows: $A_N = 13.22$ G, $A_H^\beta = 11.87$ G for one diastereomer and $A_N = 13.20$ G, $A_H^\beta = 9.58$ G for the other. For the diastereomer with $A_H^\beta = 11.87$ G, the four ^{1}H's at C-3 and C-4 and the three methyl ^{1}H's were assumed to have hyperfine splittings of 0.2 G; they were assumed to have hyperfine splittings of 0.16 G for the diastereomer with $A_H^\beta = 9.58$ G. Other conditions of the simulation were as for Figure 1 as appropriate. The dots are experimental data, and the solid line is fitted data.

example, the low field indicated by the arrow in Figure 1) be symmetric about the baseline, which is clearly at odds with the experimental spectrum. An equal-population model of two isomers to explain the EPR spectrum *can* be obtained if the apparent line widths of the two diastereomers are unequal. However, there is no physical mechanism for a single spin one-half hydrogen hyperfine splitting that could produce two EPR spectra with unequal populations and unequal line widths.

We turn now to the models with two diastereomers. An immediate question is whether the diastereomers have different *g*-values or whether they have different hyperfine splittings? Originally our interpretation favored a *g*-value difference but experiments carried out at the Medical College of Wisconsin National EPR Center on these aminoxyls at S-band (3.5 GHz) and L-band (1.1 GHz) showed that a *g*-value difference could not be the reason, as these EPR spectra were centered at different fields: the EPR spectrum of aminoxyls **14** and **17** taken at S-band and L-band (not shown) were *identical* with those acquired at X-band (9.5 GHz). Hence, the separation of the two diastereomers must be due to different hyperfine tensors. EPR spectra depicted in Figures 2 and 3 and Table 1 show that all data are well fitted by the model with both diastereomers having the same ^{14}N tensor value of ~13.2 G with one diastereomer having a ^{1}H hyperfine splitting of ~9.54 G and the other a ^{1}H hyperfine splitting of ~11.8 G.

The relative proportions of these two diastereomers are open to interpretation. Are they equal or do they differ? A decision between these two possibilities requires us to delve more deeply into the mechanisms of line width broadening in such nitroxides. The fundamental Lorentzian line width of a nitroxide is determined by the *g*- and *A*-tensors of the electron as well as the rotational correlation time for the molecule.[10b] Collisions with oxygen and other aminoxyls can broaden this line. Finally the hyperfine couplings from other paramagnetic nuclei in the molecule—four ^{1}H's at C-3 and C-4 and three methyl ^{1}H's—inhomogeneously broaden the Lorentzian to produce the apparent line width observed. If we start from the assumption that rotational correlation times and tensor properties are identical, and that the collision broadening is the same for both diastereomers, then the Lorentzian line widths must be identical as well as the observed line width. However, one might argue that the different ^{1}H hyperfine splittings of the two diastereomers (9.5 and 11.8 G) result from slightly different electron distributions around the ring. This could make the apparent line widths of one diastereomer different from the other due to slightly different unresolved hyperfine splittings—even if the fundamental physical processes that determined the basic Lorentzian line were the same. Experimentally, the greater apparent line width is associated with the diastereomer that has the larger hyperfine splitting, which means that electron density is increased on the single ^{1}H at the 2-position relative to the other diastereomer. Generally, for nitroxides if the electron density increases at one point in the ring then

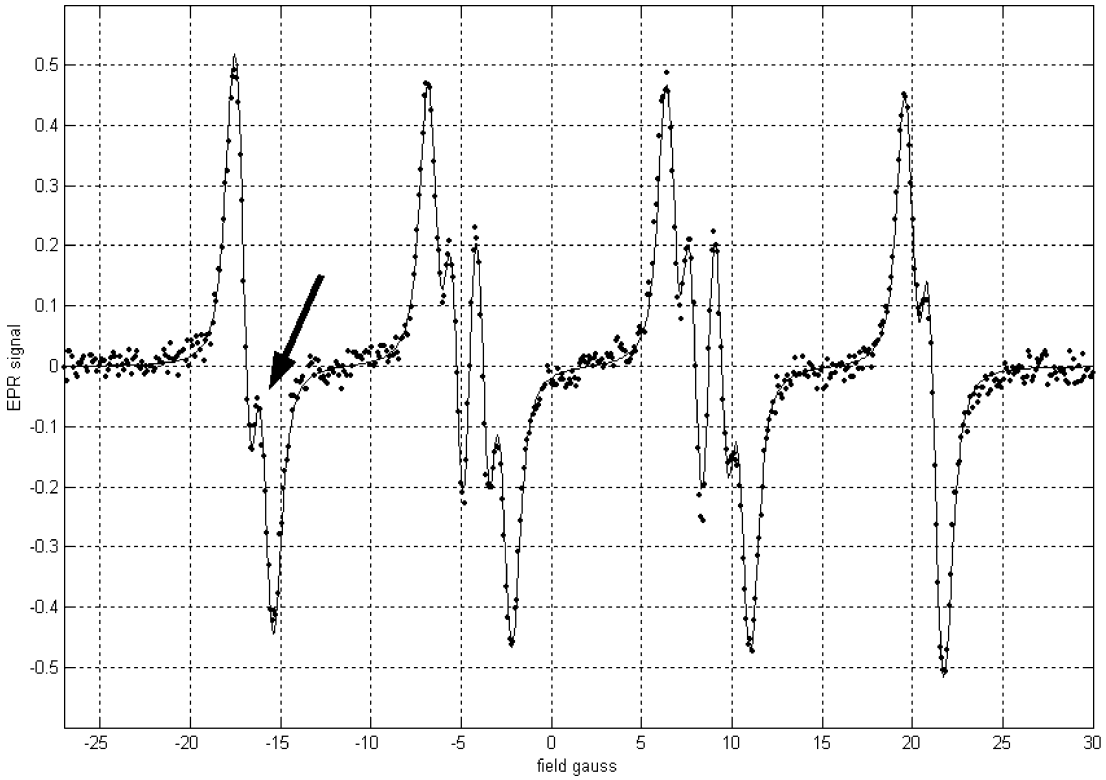

FIGURE 3. EPR spectrum of aminoxyl **17** fitted with a model that assumes there are two diastereomers with unequal populations but with the individual Lorentzian line widths allowed to float. Fitted parameters were the following: $A_N = 13.22$ G, $A_H{}^{\beta} = 11.77$ G for one diastereomer and $A_N = 13.21$ G, $A_H{}^{\beta} = 9.47$ G for the other. Other conditions were as for Figure 1 as appropriate.

the electron densities increase at all the other positions.[11] In principle this could also lead to significantly different *g*-values and particularly ^{14}N hyperfine splittings for isomers; however, simulations do not bear this out as the *g*-values of the isomers are identical.

We modeled the spectra of the diastereomers including the (unresolved) hyperfine splittings of the four ^{1}H's at C-3 and C-4 and three methyl ^{1}H's. The values of the ^{1}H tensors, 0.2 G for one diastereomer and 0.16 G for the other, were in the same relative ratio as the 2-position ^{1}H splittings (∼11.8/∼9.5).[11] To test whether there were equal populations of the two diastereomers we fitted the experimental EPR spectrum with the diastereomers fixed equal in proportion and allowed the Lorentzian line widths to float; then the same fit was done but the diastereomer proportions and the Lorentzian line widths were allowed to float. Because we expect the Lorentzian line widths of both species to be similar, the fit that puts their Lorentzians closer in value will be the better model. We found that the model with unequal proportions found Lorentzians of 0.448 and 0.485 G for the lower hyperfine and higher hyperfine diastereomer, respectively. The equal proportion model found widths of 0.550 and 0.402 G for the two diastereomers. As we expect the Lorentzians to be nearly equal, differing only by small hyperfine tensor anisotropies, these findings favor the unequal population case. All data in Table 1 have been obtained with this model.

It is important to note that the hyperfine tensors for the whole range of compounds were essentially identical. We conclude that a γ-splitting interpretation is wrong for these data.

Rate constants

Apparent rate constants for the reaction of $O_2^{\bullet-}$ with nitrones **7**−**12** were estimated by using ferricytochrome *c* as a competitive inhibitor. Ferricytochrome *c* (cyto-Fe^{3+}) was chosen for these experiments, since the rate constant for its reaction with $O_2^{\bullet-}$ is known[12] and neither ferricytochrome *c* nor ferrocytochrome *c* interfere with the EPR spectrum of aminoxyls **13**−**18**. Typically, reaction of either nitrone **7** or ferricytochrome *c* with $O_2^{\bullet-}$ can be expressed as:

$$O_2^{\bullet-} + \text{nitrone } \mathbf{7} \rightarrow \text{aminoxyl } \mathbf{13} \quad (1)$$

$$O_2^{\bullet-} + \text{cyto-}Fe^{3+} \rightarrow \text{cyto-}Fe^{2+} \quad (2)$$

From eqs 1 and 2, the rate of $O_2^{\bullet-}$ elimination in the presence of ferricytochrome *c* can be represented as

$$-d[O_2^{\bullet-}]/dt = k_{app}[\mathbf{7}][O_2^{\bullet-}] + k_{cyto-Fe}{}^{2+}[\text{cyto-}Fe^{3+}][O_2^{\bullet-}] \quad (3)$$

In the absence of ferricytochrome *c*, the formation of the spin trapped adduct can be described as

(11) Bales, B. L.; Blum, R. A.; Mareno, D.; Peric, M.; Halpern, H. J. *J. Magn. Reson.* **1992**, *98*, 299−307.

(12) Koppenol, W. H.; Van Buuren, K. J. H.; Butler, J.; Braams, R. *Biochim. Biophys. Acta* **1976**, *449*, 157−168.

$$d[\mathbf{13}]/dt = k_{app}[\text{nitrone } \mathbf{7}][O_2^{\bullet -}] \quad (4)$$

By dividing eq 4 into eq 3 and rearranging the terms, the competing reactions become

$$(-d[O_2^{\bullet -}]/dt)/(d[\mathbf{13}]/dt) = 1 + k_{cyto-Fe}{}^{2+}[\text{cyto-Fe}^{3+}]/k_{app}[\text{nitrone}\mathbf{7}] \quad (5)$$

In these kinetic experiments, the concentration of nitrone **7** is in large excess compared to the rate of $O_2^{\bullet -}$ production. Therefore, the relative concentration of aminoxyl **13**, as determined by EPR spectral peak height, is directly related to k_{app} and $k_{cyto-Fe}{}^{2+}/k_{app}$, the rate constants for the reaction of $O_2^{\bullet -}$ by nitrone **7** and ferricytochrome *c*, respectively, at a given concentration of nitrone **7**. Thus, eq 5 can be represented as

$$A_o/A = 1 + k_{cyto-Fe}{}^{2+}[\text{cyto-Fe}^{3+}]/k_{app}[\text{nitrone } \mathbf{7}] \quad (6)$$

where A_o and A represent the rate of spin trapping $O_2^{\bullet -}$ in the absence and presence of ferricytochrome *c*, respectively. If the concentration of the nitrone **7** were fixed, then a plot of A_o/A versus [cyto-Fe^{3+}] produces a straight line, the slope being $k_{cyto-Fe}{}^{2+}/k_{app}$[nitrone **7**].[13] By using the known rate constant[12] for the reduction of ferricytochrome *c* with $O_2^{\bullet -}$, $k_{cyto-Fe}{}^{2+} = 1.1 \times 10^6$ M^{-1} s^{-1} at pH 7, the k_{app} for nitrone **7** can be calculated.[14] Rate constants for the reaction of $O_2^{\bullet -}$ with nitrones **7**−**12** are listed in Table 2.

The phagosome of macrophages and neutrophils is acidic, ranging from 5.8 to 6.5.[15] Since $O_2^{\bullet -}$ is secreted into this vacuole where this free radical has been spin trapped,[16] we decided to determine the rate constant for the reaction of nitrone **11** with $O_2^{\bullet -}$ under acidic conditions. For these experiments, NADPH/FMN was used as a source of $O_2^{\bullet -}$ and ferricytochrome *c* as a competitive inhibitor. As was previously found for nitrone **1**,[6a] at an acidic pH, e.g., pH ∼5, where the concentration of $HO_2^{\bullet}$ is considerably greater than at pH 7.0 (pK_a $HO_2^{\bullet}/O_2^{\bullet -}$ = 4.8),[17] the rate constant increased from 75 M^{-1} s^{-1} at pH 7.0 to 239 M^{-1} s^{-1} at pH 5.0 (Table 3).

Next, we investigated the stability of aminoxyls **13**−**18** in phosphate buffer at pH 7.0 and pH 7.4 (Table 4). Surprisingly, these aminoxyls exhibited long lifetimes for nitroxides with a hydrogen atom at C1 (Scheme 3). One rather interesting finding is that aminoxyl **15** had a half-life of about 50% of that found for the other aminoxyls shown in Table 4. Why the *n*-butyl ester group promotes rapid loss of nitroxide signal, either through hydrolysis or disproportionation,[6] is currently under investigation.

Conclusions

Herein, we describe the reaction of nitrones **7**−**12** with $O_2^{\bullet -}$. Unlike nitrones **1** and **4**, these spin traps are very stable, slow to hydrolyze/oxidize to spurious aminoxyls. In fact, nitrones **8**, **11**, and **12** are solids and appear to be resistant to air oxidation in aerobic phosphate buffers, a significant limitation with nitrones **1** and **4**. EPR spectra of aminoxyls **13**−**18**, derived from the reaction of $O_2^{\bullet -}$ with nitrones **7**−**12**, are similar and appear to reflect the composite of different diastereomers of these aminoxyls. Of particular interest was the finding that rate constants for the reaction of nitrones **7**−**12** with $O_2^{\bullet -}$ were comparable to that found for nitrone **4**.[8c] However, the stability of the corresponding aminoxyls in phosphate buffer exceeded that reported for aminoxyl **5**.[8c] Finally, EPR spectra of aminoxyls **13**−**18** exhibit a greater signal-to-noise ratio than that found for aminoxyl **5**. The small signal-to-noise ratio of aminoxyl **5** is the result of additional hyperfine splitting associated with the phosphorus atom located at the C5 position.[8c] When one considers all data presented herein it appears that 5-methoxycarboxyl-5-methyl-1-pyrroline *N*-oxide **8,** 5-*tert*-butoxycarboxyl-5-methyl-1-pyrroline *N*-oxide **11,** and 5-*iso*-butoxycarboxyl-5-methyl-1-pyrroline *N*-oxide **12** are the best spin traps for reporting biologically generated $O_2^{\bullet -}$.

TABLE 2. Rate Constants for Spin Trapping $O_2^{\bullet -}$ by Nitrones[a]

nitrone	k_{app} (M^{-1} s^{-1}), pH 7.0
[**7**]	74.5 ± 6.4
[**8**]	78.5 ± 2.1
[**9**]	81.3 ± 6.4
[**10**]	73.5 ± 4.9
[**11**]	77.0 ± 5.0[b]
[**12**]	76.5 ± 4.9

[a] Xanthine/xanthine oxidase was used as a source of $O_2^{\bullet -}$. Experiments (n = 6) were conducted in 50 mM Chelexed potassium phosphate buffer containing DTPA (1 mM). Superoxide was generated at a rate of 1−2 μM/min. [b] The rate constant for the spin trapping of $O_2^{\bullet -}$ by nitrone [**11**] has been published elsewhere.[9e]

TABLE 3. Effect of pH on the Rate Constant for Spin Trapping $O_2^{\bullet -}$ by Nitrone [11][a]

nitrone	k (M^{-1} s^{-1}), pH 7.0	k (M^{-1} s^{-1}), pH 5.0
[**11**]	75.0 ± 10.5	239.2 ± 10.5

[a] The source of $O_2^{\bullet -}$ was FMN = 300 μM, NADPH = 300 μM in 50 mM Chelexed potassium phosphate buffer containing DTPA (1 mM) at pH 7.0 (n = 6); FMN = 150 μM, NADPH = 150 μM in 50 mM Chelexed potassium phosphate buffer containing DTPA (1 mM) at pH 5.0 (n = 6).

TABLE 4. Half-Life of Aminoxyls[a]

aminoxyl	$t_{1/2}$ (min), pH 7.0	$t_{1/2}$ (min), pH 7.4
[**13**]	21.8 ± 2.1	24.6 ± 2.7
[**14**]	20.8 ± 1.2	18.5 ± 1.3
[**15**]	8.9 ± 1.7	8.9 ± 1.7
[**16**]	17.3 ± 0.9	16.0 ± 2.0
[**17**]	22.0 ± 3.9	22.8 ± 0.9[b]
[**18**]	23.8 ± 3.7	21.0 ± 2.7

[a] Xanthine/xanthine oxidase was used as a source of $O_2^{\bullet -}$. Experiments (n = 6) were conducted in 50 mM Chelexed potassium phosphate buffer containing DTPA (1 mM). Superoxide was generated at a rate of 1 μM/min. After 8 min, SOD (30 U/mL) was added to terminate the reaction. [b] The half-life for aminoxyl [**17**] has been published elsewhere.[9e]

Experimental Section

General. Diethylenetriaminepentaacetic acid (DTPA), NADPH (nicotinamide adenine dinucleotide phosphate), FMN

(13) Tsai, P.; Elas, M.; Barasca, A. D.; Barth, E. D.; Mailer, C.; Halpern, H. J.; Rosen, G. M. *J. Chem. Soc., Perkin Trans. 2* **2001**, 875−880.

(14) (a) Asada, K.; Takahashi, M.; Nagate, M. *Agric. Biol. Chem.* **1974**, *38*, 471−473. (b) Tsai, P.; Pou, S.; Straus, R.; Rosen, G. M. *J. Chem. Soc., Perkin Trans. 2* **1999**, 1759−1763.

(15) (a) Lukacs, G. L.; Rotstein, O. D.; Grinstein, S. *J. Biol. Chem.* **1991**, *266*, 24540−24548. (b) Grinstein, S.; Furuya, W. *Am. J. Physiol.* **1988**, *254*, C272−C285.

(16) Pou, S.; Rosen, G. M.; Britigan, B. E.; Cohen, M. S. *Biochim. Biophys. Acta* **1989**, *991*, 459−464.

(17) (a) Behar, D.; Czapski, G.; Rabani, J.; Dorfman, L. M.; Schwarz, H. A. *J. Phys. Chem.* **1970**, *74*, 3209−3212. (b) Bielski, B. H. J. *Photochem. Photobiol.* **1978**, *28*, 645−649.

(flavin mononucleotide), ferricytochrome *c*, xanthine, and xanthine oxidase (EC 1.1.3.22) were purchased from Sigma Chemical Company (St. Louis, MO). Superoxide dismutase (SOD) was obtained from Boehringer Mannheim (Indianapolis, IN). Chelex 100 ion-exchange resin was purchased from Bio-Rad (Richmond, CA). All other chemicals were of reagent grade unless indicated otherwise.

Generation of Superoxide. Superoxide was generated for spin trapping experiments, using one of two sources: (a) xanthine/xanthine oxidase at pH 7.0 or pH 7.4 and (b) NADPH and FMN at pH 5.0 and 7.0. For data in Table 2, $O_2^{\bullet-}$ production was realized by mixing xanthine (400 μM) and sufficient xanthine oxidase in sodium phosphate buffer (50 mM, Chelexed, at pH 7.0 containing 1 mM DTPA) to reach a rate of $O_2^{\bullet-}$ generation of 1−2 μM/min. Control experiments contained SOD (30 U/mL). For data in Table 3, $O_2^{\bullet-}$ production was achieved by mixing NADPH (300 or 150 μM) and FMN (300 or 150 μM) in sodium phosphate buffer (50 mM, Chelexed) containing DTPA (1 mM), at either pH 5.0 or pH 7.0, containing 1 mM DTPA.

Spin Trapping Superoxide. EPR spectra of aminoxyls **13**−**18**, derived from the reaction of $O_2^{\bullet-}$ with nitrones **7**−**12**, were recorded on an EPR spectrometer. Nitrones (50 mM) were added to each of the $O_2^{\bullet-}$ generating systems. Reaction mixtures were transferred to a flat quartz cell, fitted into the cavity of the EPR spectrometer, and spectra were recorded at room temperature. Instrumentation settings were the following: microwave power, 20 mW; modulation frequency, 100 kHz; modulation amplitude, 0.5 G; response time, 0.5 s; and sweep, 12.5 G/min. Hyperfine splitting constants are presented in Table 1.

Rate Constants for Spin Trapping Superoxide. Apparent rate constants for the spin trapping of $O_2^{\bullet-}$ by nitrones **7**−**12** were estimated by using the model $O_2^{\bullet-}$ generating system of xanthine/xanthine oxidase. In a typical experiment, the reaction mixture contained nitrone **7** (60 mM), xanthine (400 μM), and sufficient xanthine oxidase to generate 1 μM/min of $O_2^{\bullet-}$ as determined by the SOD-inhibitive reduction of ferricytochrome *c* (80 μM) at 550 nm, using an extinction coefficient of 21 mM^{-1} cm^{-1}, as described in the literature.[18]

Ferricytochrome *c* (0−23 μM) was used as a competitive inhibitor. Reaction mixtures were immediately transferred to an EPR flat quartz cell and introduced into the cavity of the EPR spectrometer. EPR spectra were recorded at room temperature 3 min after the reaction was initiated by the addition of xanthine oxidase. Rate constants are presented in Tables 2 and 3.

Estimation of the Half-Life of Aminoxyls 13−18. The half-life of aminoxyls **13**−**18** was determined by monitoring the decrease in the first line of the EPR spectrum of these aminoxyls as a function of time. In a typical experiment, the reaction mixture contained nitrone **7** (50 mM), xanthine (400 μM) in potassium phosphate buffer (Chelexed, 50 mM, pH 7.4, 1 mM DTPA, 1 mM EGTA), and sufficient xanthine oxidase, generating $O_2^{\bullet-}$ at 1 μM/min, for 8 min, and then SOD (30 U/mL) was added. The reaction mixture was immediately transferred to an EPR flat quartz cell and introduced into the cavity of the EPR spectrometer. EPR spectra were continually recorded for 60 min. Data are presented in Table 4.

Acknowledgment. This research was supported in part by grants from the National Institutes of Health, RR-12257, EB-2034, and GM-65944. We wish to thank Dr. Chris Felix of The National Biomedical EPR Center of the Medical College of Wisconsin in Milwaukee, WI, for access to the L- and S-band spectrometers.

Supporting Information Available: Experimental procedures for the preparation of nitrones **7**−**12**. This material is available free of charge via the Internet at http://pubs.acs.org.

JO0350413

(18) Kuthan, H.; Ullrich, V.; Estabrook, R. *Biochem. J.* **1982**, *203*, 551−558.